



Minerva Access is the Institutional Repository of The University of Melbourne

Author/s:

Mariani, M;Holz, A;Veblen, TT;Williamson, G;Fletcher, MS;Bowman, DMJS

Title:

Climate Change Amplifications of Climate-Fire Teleconnections in the Southern Hemisphere

Date:

2018-05-28

Citation:

Mariani, M., Holz, A., Veblen, T. T., Williamson, G., Fletcher, M. S. & Bowman, D. M. J. S. (2018). Climate Change Amplifications of Climate-Fire Teleconnections in the Southern Hemisphere. *Geophysical Research Letters*, 45 (10), pp.5071-5081. <https://doi.org/10.1029/2018GL078294>.

Persistent Link:

<https://hdl.handle.net/11343/284018>

Mariani Michela (Orcid ID: 0000-0003-1996-3694)  
Holz Andres (Orcid ID: 0000-0002-8587-2603)  
Williamson Grant, James (Orcid ID: 0000-0002-3469-7550)  
Fletcher Michael-Shawn (Orcid ID: 0000-0002-1854-5629)  
Bowman David (Orcid ID: 0000-0001-8075-124X)

**TITLE: *Climate change amplifications of climate-fire teleconnections in the Southern Hemisphere***

Mariani, Michela<sup>1\*</sup>; Holz, Andrés<sup>2\*</sup>; Veblen, Thomas T.<sup>3</sup> ; Williamson, Grant<sup>4</sup>; Fletcher, Michael-Shawn<sup>1</sup> and Bowman, David M.J.S.<sup>4</sup>

<sup>1</sup>School of Geography, University of Melbourne, Victoria, Australia

<sup>2</sup>Department of Geography, Portland State University, Oregon, United States of America

<sup>3</sup>Department of Geography, University of Colorado Boulder, Colorado, United States of America

<sup>4</sup> School of Natural Sciences, University of Tasmania, Tasmania, Australia

\*Corresponding authors

WORD COUNT: 3955

## **ABSTRACT**

This is the author manuscript accepted for publication and has undergone full peer review but has not been through the copyediting, typesetting, pagination and proofreading process, which may lead to differences between this version and the [Version of Record](#). Please cite this article as doi: [10.1029/2018GL078294](https://doi.org/10.1029/2018GL078294)

Recent changes in trend and variability of the main Southern Hemisphere climate modes are driven by a variety of factors, including increasing atmospheric greenhouse gases, changes in tropical sea-surface temperature and stratospheric ozone depletion and recovery. One of the most important implications for climatic change is its effect via climate teleconnections on natural ecosystems, water security and fire variability in proximity to populated areas, thus threatening human lives and properties. Only sparse and fragmentary knowledge of relationships between teleconnections, lightning strikes, and fire is available during the observed record within the Southern Hemisphere. This constitutes a major knowledge gap for undertaking suitable management and conservation plans. Our analysis of documentary fire records from Mediterranean and temperate regions across the Southern Hemisphere reveals a critical increased strength of climate-fire teleconnections during the onset of the 21<sup>st</sup> century including a tight coupling between lightning-ignited fire occurrences, the upward trend in the Southern Annular Mode and rising temperatures across the Southern Hemisphere.

## 1. INTRODUCTION

Fire is a key Earth system process determining global vegetation distribution [*Bond et al., 2005*], modulating the carbon cycle [*Liu et al., 2015*], and influencing the climate system [ *Bowman et al., 2009*]. Documenting mechanisms behind climate-fire dynamics is critical for understanding the future of Earth's ecosystems under projected climate and fire change scenarios [*Abatzoglou and Williams, 2016; Jolly et al., 2015; Westerling et al., 2006*]. Given the large variety of biomes and fire regimes around the Southern Hemisphere (SH) [*Bond et al., 2005; Bowman et al., 2009; Enright and Hill, 1995; Murphy et al., 2013*], it is crucial to understand how fire activity responds to climate

variability within different vegetation contexts and climatic frameworks, and how such dynamics are being altered by climate change. Here we (1) present the first hemispheric-scale compilation of relationships between large-scale climate modes (e.g. El Niño Southern Oscillation, Southern Annual Mode and Indian Ocean Dipole) and documentary records of lightning- and human-ignited fires for the past 30-50 years and (2) present the first synthesis of climate change-mediated impacts on these climate-fire teleconnections across temperate and Mediterranean biomes of Chile, Argentina, South Africa and Australia (Figure 1a).

Across the Earth, variability in fire occurrence and spread is determined by the confluence of sufficient and dry fuel, an ignition source, and suitable weather for burning [Bradstock, 2010; Krawchuk *et al.*, 2009]. In moist temperate forest areas, since there is abundant biomass to burn (Figure 1b), fire activity through time is controlled by fuel moisture content (i.e. climate) and ignitions (lightning and humans) [Bradstock, 2010; Cochrane, 2003; McWethy *et al.*, 2013; Pausas and Ribeiro, 2013]. In contrast, fires in drier temperate biomes (e.g. Mediterranean-type ecosystems) are both moisture-limited and biomass-limited (Figure 1b). Increased fire activity in Mediterranean-type ecosystems is sensitive to quasi-annual antecedent rainfall pulses, whereas concurrent droughts and/or hot-dry winds tend to be the key driver of fire activity in temperate forests [Moritz *et al.*, 2012]. Hence predicting future fire activity hinges partly on understanding the impact of climate conditions, mediated by large-scale climate drivers, on landscape flammability via vegetation type and inherent fuel traits [Krawchuk *et al.*, 2009; Moritz *et al.*, 2012]. The SH features extensive areas of both Mediterranean-type and temperate forest ecosystems, both hosting endemic and fire-sensitive Gondwanan plant species, embedded in fire-prone vegetation (e.g. eucalypt forests of southeast

Australia; introduced pine plantations in Central Chile) [Hennessey *et al.*, 2005]. In these settings human ignitions are known to increase with intermediate population densities, but most fires are aggressively fought except those uncontrollable due to extreme weather conditions [Bowman *et al.*, 2017].

Despite the acknowledged importance of various climate modes in modulating fire weather across the SH, analyses of their influence on SH fire activity are few in number, focus on one or few climate modes and are spatially fragmented [Cai *et al.*, 2009; Holz and Veblen, 2011; Holz *et al.*, 2012; Mariani *et al.*, 2016] – hence a hemispheric synthesis of climate-fire teleconnections is overdue. Here we consider the three large-scale climate modes operating at inter-annual and decadal scales in the Southern Hemisphere – the Southern Annular Mode (SAM), the El Niño Southern Oscillation (ENSO), the Indian Ocean Dipole (IOD) (Figure 1c,d,e) – to a) identify the individual most important climate index influencing fire activity by vegetation types within Mediterranean-type and temperate forest ecosystems across the SH and b) quantify the past variability of teleconnections between climate modes and fire activity throughout the end of the 20<sup>th</sup> and the start of the 21<sup>st</sup> century.

This work also aims to identify the effects of the above-mentioned climatic change on the teleconnections between climate modes and natural (lightning-ignited) fire occurrences across the Southern Hemisphere. Although lightning strikes constitute the most important natural ignition source for wildfires, they only account for a small proportion of total fire occurrence in many regions on Earth [Bowman *et al.*, 2009]. Nonetheless, under warmer conditions it is likely that the potential for lightning-ignited wildfires will increase in response to climate change [Abatzoglou *et al.*, 2016; Williams,

2005]. There have been few attempts to understand the implications of increased flash rate on fire activity, principally area burnt from short-term coupled satellite data and climate models [Goldammer and Price, 1998; Krause et al., 2014; Price and Rind, 1994], and there is a dearth of information on the hemisphere-wide relationship between actual lightning-ignited fires and climate trends. To address this important knowledge-gap, we compiled a hemispheric-scale documentary dataset of natural (lightning-ignited) wildfire occurrences, testing the connection between trends in lightning-ignited fires and (1) rising SH temperature and (2) variability in the leading climate modes throughout the late 20<sup>th</sup> and early 21<sup>st</sup> centuries.

## 2. METHODS

### 2.1 Fire and climate records and climate indices

Fire occurrence data were obtained through local administrative databases from four countries within the Mediterranean-type and temperate forest regions of the Southern Hemisphere: Chile, Argentina, Australia and South Africa (Figure 1). Information on the datasets collected and the sources are presented in Supporting Information (SI) Appendix Table S1. We define a fire season year (extending from the austral spring—early September—through early fall – late March) by the year in which the fire season starts—e.g., fire season 1951/1952 = 1951). Two (per fire season) fire-regime metrics were used to represent annual-scale fire activity: number of occurrences and area burnt per fire season, including both human-set and lightning-set fires (separately and merged). Prescribed burns and arson fires were excluded from all datasets prior to analyses, thus we used only accidental and unplanned fire events. To minimize the effect of errors in area burnt measurements and small human-set fires, only fire events larger than 5 hectares were included in the analyses. To account for differences in climate-fire

mechanisms in each biome, fire data were separated by vegetation type: herb/grass-dominated versus tree-dominated vegetation within the broad climate study regions.

## 2.2. Statistical analyses

Simple and partial Pearson correlations, scatterplot analyses and linear regression models were conducted to examine the spatio-temporal relationships of past and future wildfire occurrences and area burnt to variability in climate modes. Time-series were tested for normality using the Shapiro-Wilk normality test [Shapiro and Wilk, 1965]. If skewed time-series were identified, a log-transformation was performed prior to correlation analyses. A simple correlation matrix was created using all the fire activity data (occurrences and area burnt) to test whether fire activity was correlated with same-year climate conditions and climate modes/variables in each study region. A significance test using a 0.9 confidence level was run in the *corrplot* package [Wei and Simko, 2016] in R [Team, 2013]. Interactions amongst climate modes involve complex feedbacks and variable interaction patterns in space and time [Cai et al., 2011; Fogt et al., 2009; Meyers et al., 2007; Risbey et al., 2009]. To account for the possible co-dependence of climate indices in modulating fire activity across the studied regions, partial correlations were calculated using simple (Pearson) correlations of the residuals of pairs of linear regression models: fire metric (e.g. area burnt in woody vegetation in South Africa) ~ climate mode 1 (e.g. IOD) + climate mode 2 (e.g. ENSO) and climate mode 3 (e.g. SAM) ~ climate mode 1 (e.g. IOD) + climate mode 2 (e.g. ENSO). In this way, two climate modes (e.g. IOD and ENSO) were set as control variables for the relationship between fire activity and the remaining climate mode (e.g. SAM).

To achieve a hemispheric synthesis of ignition patterns, fire occurrences from all the regions were summed as departures (in SD units, i.e. z-scores) and run through the

same partial correlation procedure. A summary table of the highest significant partial correlation values (i.e. seasonal or annual) per region, biome, and dominant vegetation type is presented in Table 1. A table with the highest significant simple Pearson correlation values is also presented (SI Table S3). A spreadsheet listing all the simple and partial correlation coefficients for all the study regions and metrics is available in SI (additional external table). Correlation matrices by region are presented in SI Figure S2a and 2b. Barplots showing the comparison of Pearson correlation coefficients between simple and partial correlations are presented in Figure S6.

To analyse changes in the patterns of ignition directly related to climate variability and change at a hemispheric scale between the 21<sup>st</sup> (2000-2014) and 20<sup>th</sup> (1958-1999) centuries, only the number of lightning-lit fires (i.e. as opposed to intra-region, idiosyncratic and complex socio-ecological ignition patterns), and not the area burnt, were considered in the statistical analyses. In this case, due to the low number of observations by year, herbaceous and woody vegetation types were combined. Simple Pearson correlation coefficients between climate indices and SH summed fire occurrences (all unplanned human fires and lightning-ignited fires) were measured on either the full and split time-series. To quantify the relationship between observed warming on fire occurrence across the SH, summed fire occurrence records from all the analysed regions (and combined vegetation types) in the SH were compared against hemispheric-scale annual temperature. To minimise the issues deriving from an uneven distribution of data points in the 20<sup>th</sup> and 21<sup>st</sup> centuries, a randomised simple correlation method was employed using 14 years in the 20<sup>th</sup> century ( $n=21^{\text{st}}$  century) that were chosen through 100 random combinations (Supporting Information TableS3, Document S3).

Lastly, to project the impact of SAM on fire occurrence under increasing greenhouse gases concentrations over the remaining of the 21<sup>st</sup> century, a simple linear model of SH fire occurrences against the summer SAM index projection (data from [McLandress *et al.*, 2011; Thompson *et al.*, 2011]).

### **3. RESULTS AND DISCUSSION**

#### **3.1 Climate modes and variability in the occurrence and extent of fire across the Southern Hemisphere**

Our measure of same-year correlation coefficients between seasonal climate mode indexes and a) total annual wildfire activity (human- [i.e. unplanned burns only] plus lightning- lit fires) and b) lightning-lit fires only, provides insights on the leading modes of fire variability in each study region. The associations of the three climate modes with fire occurrence and area burnt, from all ignition sources and lightning alone, are described below, with subsequent sections considering the effects of ENSO, IOD and SAM separately. Differences between patterns of human- and lightning- ignited fires were not addressed in this work, as they are idiosyncratic to the different cultures and regions (e.g. motives and timing of intentional or accidental burning) and require a research design targeting human behaviour.

ENSO (NIÑO 3.4 Index) is significantly positively correlated with wildfire activity in temperate Australia (SEAUS; i.e. number of fires and area burnt in both vegetation types), Mediterranean Chile (CHMEDI; i.e. area burnt in both vegetation types), western Mediterranean Australia (WMEDIAUS; i.e. number of fires and area burnt in woody vegetation) and temperate South America (TEMPSA; i.e. area burnt in woody

vegetation). The highest partial correlation coefficient values between fire and ENSO were consistently found across regions in spring in the temperate regions, while they were found in the antecedent autumn in the Mediterranean regions (Figure S2). ENSO is also significantly associated to lightning-ignited fire occurrences in SEAUS and CHMEDI in summer (for both vegetation types combined [see Methods section]; Table 1b).

The IOD shows significant partial correlations with the fire activity metrics in all vegetation types across all temperate regions during spring, summer and annually, and also in some Mediterranean regions with both herbaceous and woody vegetation (Table 1a). In CHMEDI and EMEDIAUS, the IOD displays negative partial correlation coefficients with the fire metrics, whereas positive values are observed in all the other regions. Significant positive correlations were also found with natural fire activity across Australia during spring.

The SAM Index shows high significant positive correlations with fire activity from all ignition sources in all regions and vegetation types (Table 1a). High partial correlation coefficients were found in spring and summer in the temperate regions, whereas the highest correlation coefficients in the Mediterranean regions were found especially in winter and annually. SAM has a significant positive correlation with lightning-lit fires for all regions (except SEAUS) particularly during summer and annually (Table 1b). Accordingly, our results indicate that SAM in the same-year summer and spring seasons plays a key role in modulating unplanned fire activity (occurrences and area burnt) across all the studied regions (Figure 2), especially across temperate forests in the SH (Table 1).

We assessed whether SAM, as the most influential climate mode across all study regions, had an impact on the combined record of all fire occurrences (number of fires) from all ignition sources in all vegetation types and across all regions that had separately shown positive correlation to the summer SAM Index (CHMEDI, WMEDIAUS, SAFR, TEMPSA, WTAS). SAM is positively correlated to fire occurrence of all regions, from all ignition sources and vegetation types combined ( $r=0.61$ ;  $p\text{-value}<0.001$ ; Figure 2a and SI Figure S4). These simple correlation coefficient values remain high and upward trends in teleconnections between SAM and fire occurrence over the SH are observed during the 20<sup>th</sup> and early 21<sup>st</sup> centuries ( $r=0.58$  and  $r=0.52$  respectively), with higher dispersion from the mean during in the early 21<sup>st</sup> century (Figure 2b). These results are supported by our randomised correlation method results (Table S3). Based on the strong linear relationship between observed summer SAM index and SH fire occurrence (i.e. number of fires) (Figure 2a), projected results on the relationship between both time-series show a persistent increasing trend throughout the 21<sup>st</sup> century, reaching up to 8-10 standard deviations from the historical mean occurrence in fire (Figure 2d).

Results indicate an overall tight and positive association between SH temperature and fire occurrence, with a persistent upward trend over time ( $r=0.54$ ;  $p\text{-value}<0.001$ ; Figure 3a). The warming-fire occurrence relationship is substantially stronger during early 21<sup>st</sup> century than the 20<sup>th</sup> century ( $r=0.64$  vs.  $r=0.12$ ,  $p\text{-value}<0.05$ ). Moreover, the SAM and IOD indexes (see all seasonal  $r$ -values in SI Figure S5) display a strong significant correlation with the number of lightning-lit fires combined across the SH, with tighter relationship and increased departure from the mean during the early part of the 21<sup>st</sup> than during the 20<sup>th</sup> centuries (Figure 3c, d).

### 3.2. ENSO: the 'Pacific' mode

Our results from the partial correlations analysis confirm existing literature supporting the importance of ENSO in driving fire activity in SEAUS, CHMEDI, WMEDIAUS and TEMPISA (Table 1), though we note an absence of a significant correlation (either positive or negative) between ENSO and the summed SH fire occurrences from all ignition sources (SI Figure S4 and S5) in all vegetation types. A significant relationship between ENSO and fire activity has been previously reported for some of the study regions used here based on both documentary records [ *Holz and Veblen, 2012; Mariani et al., 2016; Nicholls and Lucas, 2007*] and tree-ring fire-scar reconstructions [ *Veblen et al., 1999*] and sedimentary (charcoal peaks) records [ *Holz and Veblen, 2012*].

Notwithstanding the lack of a significant correlation between fire occurrences and ENSO across the entire SH (i.e. summed records; SI Figure S4 and S5), the scatterplot presented in Figure 3 showing the split time-series (20<sup>th</sup> and 21<sup>st</sup> century separated) highlights the importance of ENSO in the current century. In this case, a more positive state of spring NIÑO3.4 (El Niño) corresponds to a large departure of fire occurrences above historical average, stepping up by about 4 standard deviations from the 20<sup>th</sup> century data point cloud (Figure 3c). The projected amplifications of El Niño and La Niña activity due to anthropogenic climate change [ *Cai et al., 2014; Cai et al., 2015; Power et al., 2013*] herald a serious threat to both fire-sensitive ecosystems and the ever-expanding flammable bush- or wild-urban interface [ *Bowman et al., 2017; Sharples et al., 2016*], presenting fire management agencies with even greater challenges than they face now. In this regard, the significant correlations of climate forcing and fire occurrence in heavily populated SEAUS and CHMEDI found in this study and elsewhere [ *Holz et al., 2012; Mariani et al., 2016*] are of concern.

### 3.3 SAM: the leading mode of fire variability in the SH

Critically, from our results it is evident that a strong departure in the positive polarity of the SAM Index above the historical mean may result in a large increase in fire occurrence by the end of the current century or earlier (Figure 2c, d). Given the importance of this climate mode in driving moisture patterns and fire activity across the mid-latitudes of the SH [ *Holz and Veblen, 2011; Holz et al., 2017; Mariani and Fletcher, 2016*], the fact that the observed trend in the SAM Index is statistically distinct from estimates of natural variability [ *Abram et al., 2014; Fogt et al., 2009*] and the projections of increased positive polarity under enhanced greenhouse gases concentrations [ *Thompson et al., 2011*], it is crucial to take this climate mode into account when addressing future projections of fire activity across the entire SH extra-tropics (Figure 2d). In terms of lightning ignitions, we identified SAM as the leading climate mode in most of the analysed regions across the SH (Table 1b, Figure 3d; see below). Anomalously large positive states of SAM were found to be linked to a great increase in number of fires during the 21<sup>st</sup> century, stepping up by at least 2 standard deviations from the 20<sup>th</sup> century data point cloud (Figure 3d). While the overall trend of these findings is unequivocal, we acknowledge that the departures projected in climate and the SAM have uncertainties associated with the use of CMIP3 models and SAM projections to 2100 (i.e. based on a GCM study; *Thompson et al. 2011* and *McLandress et al. 2011*). For instance, in the future it is highly likely that the non-linearities of the climate dynamics (linked to changes in ozone-depleting substances and concentration of greenhouse gases) will manifest more strongly, in turn affecting the reliability of projections in SAM and SAM-fire relationships.

### 3.4 IOD and SH fire activity: not only an Indian Ocean mode

Our results suggest the existence of a relatively strong correlation between IOD and variation in fire ignited from all sources and lightning across Australia (SEAUS, WTAS and WMEDIAUS) and SAFR. Positive IOD events are linked to negative precipitation anomalies across the Australian continent occasionally up to its Pacific coast [Cai *et al.*, 2009], especially when occurring in combination with El Niño events [Meyers *et al.*, 2007; Risbey *et al.*, 2009]. Our results also report for the first time, teleconnections between IOD and fires in South America (CHMEDI, SATEMP), a region that is not located within the 'classical' IOD zone of influence [Saji *et al.*, 1999] (Figure 1). Although climate mechanism and relationship between the IOD and South American rainfall have been described in the past [Chan *et al.*, 2008; Taschetto and Ambrizzi, 2012], we believe our findings are probably mostly related to the complex spatio-temporal ENSO-SAM-IOD teleconnections [Cai *et al.*, 2011], but further studies are needed. In spite of the fact that the IOD does not have a significant correlation with lightning-lit fire occurrences during the 20<sup>th</sup> century, the strong association found during the 21<sup>st</sup> century (Figure 3d) highlights the possible implication of recent climatic change and warming of the SH and the Indian Ocean (IO) [Vecchi and Soden, 2007].

### 3.5. A warmer and fiery future?

Our correlative analyses suggest a strong link between lightning-lit fires, rising hemispheric temperatures and the increasingly positive polarity of the SAM, NIÑO3.4, and IOD indexes over the 21<sup>st</sup> century (Figure 3). Climate change is projected to increase lightning strikes (cloud to ground) frequency, an important source of ignition for wildfires [Abatzoglou *et al.*, 2016; Romps *et al.*, 2014], with an estimated warming-induced increase of roughly 5–12% for every degree (°C) [Michalon *et al.*, 1999; Price

and Rind, 1994; Romps *et al.*, 2014] and up to 21.3% for the RCP85 projection (IPCC, 2014) at the end of the 21<sup>st</sup> century [Krause *et al.*, 2014]. Evidence of the warming pressure on natural fire variability is the high positive correlation coefficient between SH temperature and lightning-lit fire occurrences and the increased strength of this correlation stepping from the 20<sup>th</sup> to the 21<sup>st</sup> century under the persistent warming trend (Figure 3a,b). Importantly, lightning strikes were the cause of recent large-fire activity and carbon loss in the boreal forests of North America, suggestive of a potential positive feedback between increased lightning incidence, subsequent fire activity and the global carbon cycle [Balch *et al.*, 2017; Veraverbeke *et al.*, 2017]. In addition, increased greenhouse gases along with the effects of ozone recovery, are expected to continue to drive the SAM, the most important fire-teleconnected climate mode identified in this study. During summers the effects of ozone recovery might cancel out greenhouse forcing, whereas during the rest of the year and on an annual basis the SAM is expected to continue on its high index polarity even under ozone recovery [Thompson *et al.*, 2011].

Our results indicate a strong positive relationship between fire occurrence and positive trends in SAM, NIÑO3.4 and IOD, especially in the early 21<sup>st</sup> century (Figure 3c,d,e), and highlight a potential further increase in fire occurrence into the future related to these climate modes. Due to the tight linkages with both unplanned and natural fire occurrence and extent across the entire SH, future SAM projections under increasing greenhouse gases concentrations and global warming are alarming (Figure 2c,d and Figure 3d) [Thompson *et al.*, 2011]. In the tropical Pacific, extreme El Niño events are projected to become more frequent due to increased ocean surface warming under a rising global temperature scenario [Cai *et al.*, 2014]. This cascade of events will likely have

consequences on anthropogenic and natural fire occurrences across temperate and Mediterranean regions across the Southern Hemisphere. Moreover, in the tropical Indian Ocean (IO), climate models project a future warming pattern that features a slower warming rate in the eastern IO than in the western IO [Vecchi and Soden, 2007]. This warming pattern matches sea surface temperature conditions similar to those occurring during a positive IOD event [Saji *et al.*, 1999], that are becoming more frequent and achieving unprecedented levels in the past 30 years [Cai *et al.*, 2009]. Given the high correlations of the IOD with Australian drought and fire records, the predicted warming pattern of the IO is most likely to increasingly impact water security and fire danger across southern Australia and may impact, at a minor magnitude, the rest of the Southern Hemisphere.

Regardless of the potential feedback between several bottom-up factors such as fire-driven vegetation change, technological advances to detect and suppress fires and the increases in human ignitions, our results indicate an underlying, marked positive trend in the lightning-ignited fires. This trend is likely to continue due to projected temperature increase and the climate modes' trajectories. These findings imply the existence of a significant threat for natural ecosystems and wildland urban interfaces across the SH. For instance, landscape-scale loss of fire-sensitive ecosystems has already occurred in response to changes in fire frequency and fire–vegetation feedbacks in parts of southeast Australia [Holz *et al.*, 2014], New Zealand [Tepley *et al.*, 2017] and southern South America [Paritsis *et al.*, 2015], with concern about a future where fires become more frequent and/or extensive. Indeed, the threat posed by increasing fire occurrence is magnified by the compounding effects of direct climate change impacts on ecosystem functioning, such as post-fire growth and recovery rates (i.e. under drier and more

flammable environments) [Enright *et al.*, 2015; Tepley *et al.*, 2018]. Enormously economical and socially disastrous fires are increasingly reported around the SH (Australia, Tasmania, New Zealand, Chile) [Bowman *et al.*, 2017]. We acknowledge our analysis is limited because we have been unable to incorporate the full array of factors and the interactions that are likely to influence trends in the multifaceted climate-fire dynamic. Nonetheless, our findings highlight the capacity of climate change particularly via lightning-ignited fires and inter-annual climate modes (i.e. fire-prone phases in SAM, IOD, and ENSO) to strongly affect the Earth System.

### **ACKNOWLEDGEMENTS**

MM was supported by AINSE (Australian Institute for Nuclear Science and Engineering) Postgraduate Research Award #12039. Andrés Holz was supported by US National Science Foundation (Awards #0956552, #0966472, and #1738104) and Australian Research Council (Grant # DP110101950). We thank Lachie McCaw for providing the raw data from Western Australia. We are thankful to D. Thompson and C. McLandress for providing the SAM projections data. We also thank the Wildfire PIRE research group for insightful comments on initial results. Data can be obtained through the sources listed in Table S1 (Supporting Information).

### **AUTHOR CONTRIBUTIONS**

M.M. conducted data collection, analysis, interpretation and led the manuscript writing; A.H. conceived ideas and helped with data analysis, interpretation and manuscript editing; T.V. helped with ideas development and manuscript editing; G.W. helped with

data analysis and manuscript editing; M.-S.F. and D.B. helped with interpretation and manuscript editing. Authors declare no competing financial interests. Correspondence should be addressed to M.M. and A.H.

Author Manuscript

## FIGURES and TABLES CAPTIONS

**Figure 1 a)** Geography of the dominant inter-annual climate modes and study regions: 1- Australia, 2- South Africa and 3- South America. **b)** Conceptual model of coarse-scale controls on fire activity: fuel-limited areas tend to experience more fire due to inter-annual pulses in precipitation. In contrast, areas with more abundant fuel tend to experience more fire due to pulses of ignitions and/or fire-conducive weather conditions (modified from Moritz et al., 2012). **c)** Time series of SAM Index (Annual); **d)** NIÑO 3.4 Index (Annual); **e)** IOD Index (Annual). See methods for sources.

**Table 1** Pearson correlation coefficients ( $r$ ) for partial correlations ( $p$ -values are indicated in parentheses) between seasonal climate modes and documentary records of fire activity: unplanned— human- and lightning-ignited fires in a) and lightning-lit only events in b), by region. Table in c) shows partial correlations for the summed fire occurrences in the Southern Hemisphere. Only highest significant same-year correlation coefficients are reported (by season). Full correlation matrices between interannual climate modes and fire activity by vegetation type for each region are presented in Supporting Information (Figure S2a,b). Letters in parentheses in a) indicate the most significant fire metric ( $N$ = number of fires;  $A$ = area burnt). Region codes: CHMEDI= Mediterranean Chile, WMEDIAUS= western Mediterranean Australia, EMEDIAUS= eastern Mediterranean Australia, SAFR= Mediterranean South Africa, SEAUS= temperate southeast Australia, WTAS= western Tasmania, TEMPSA= temperate South America (Chile and Argentina). The letter  $n$  in parentheses indicates the number of years used to run Pearson correlation coefficients. N/A stands for information Not Available due to lack of data. Control variables refers to the climate modes kept constant to account for co-dependencies in their respective effect on fire activity.

**Figure 2 a)** Stacked plots of the SAM Index (summer) and the total number of wildfires in the Southern Hemisphere (black solid line; only regions with a positive correlation with the SAM Index are included in the summed record) from all ignition sources and vegetation types combined; **b)** Scatterplot of the two time-series shown in a). Colour and symbol coding refers to the 20<sup>th</sup> (blue dots) and the 21<sup>st</sup> (red triangle) centuries; **c)** Summer SAM Index projection under increasing greenhouse gases concentrations (data from Thompson et al., 2011 and *McLandress et al.*, 2011); **d)** Linear model projecting

the total (human and lightning-lit) wildfire occurrences in the SH extending to the year 2100 based on the SAM Index projection presented in c). Pearson correlation coefficients are reported in a) and b).

**Figure 3 a)** Stacked plots of the SH annual temperatures (z-scores; data from ERA-Interim Reanalysis) and the total number of lightning-lit fires recorded in the Southern Hemisphere. **b)** Scatterplot of the SH annual temperatures (z-scores; data from ERA-Interim Reanalysis) and the total number of lightning-lit fires recorded in the Southern Hemisphere; Black solid line in a) represents the summed SH number of lightning-ignited fires. Colour and symbol coding in b,c,d,e refers to the 20<sup>th</sup> (blue dots) and the 21<sup>st</sup> (red triangle) centuries. **c)** Scatterplot of the NIÑO3.4 Index (spring) and the number of lightning-lit fires across the SH; **d)** Scatterplot of the SAM Index (summer) and the number of lightning-lit fires across the SH; **e)** Scatterplot of the IOD Index (spring) and the number of lightning-lit fires across the SH.

FIGURES and TABLES

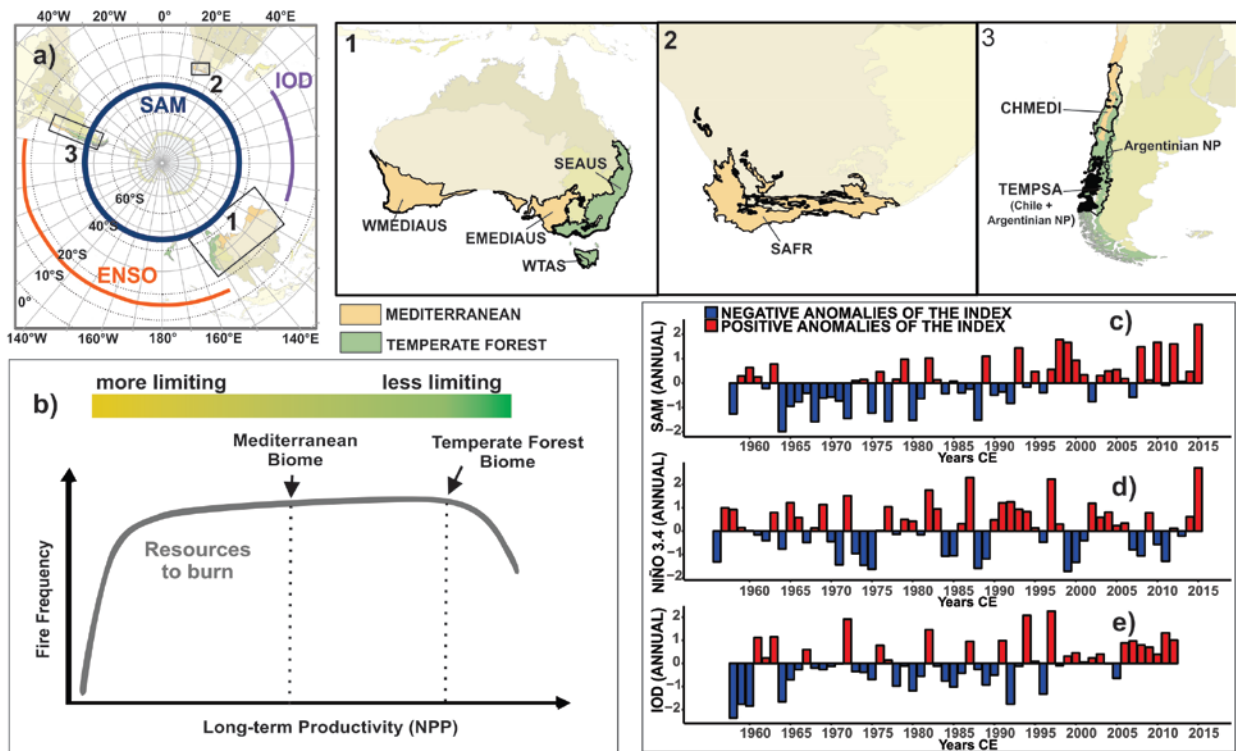


**Figure 1 a)** Geography of the dominant climate modes and study regions: 1- Australia, 2- South Africa and 3- South America. **b)** Conceptual model of coarse-scale controls on fire activity: fuel-limited areas tend to experience more fire due to inter-annual pulses in precipitation. In contrast, areas with more abundant fuel tend to experience more fire due to pulses of ignitions and/or fire-conductive weather conditions (modified from Moritz et al., 2012). **c)** Time series of SAM Index (Annual); **d)** NIÑO 3.4 Index (Annual); **e)** IOD Index (Annual). See methods for sources.

**Table 1**

Pearson correlation coefficients ( $r$ ) for partial correlations ( $p$ -values are indicated in parentheses) between seasonal climate modes and documentary records of fire activity: unplanned— human- and lightning-ignited fires in a) and lightning-lit only events in b), by region. Table in c) shows partial correlations for the summed fire occurrences in the Southern Hemisphere. Only highest significant same-year correlation coefficients are reported (by season). Full correlation matrices between interannual climate modes and fire activity by vegetation type for each region are presented in Supporting Information (Figure S2a,b). Letters in parentheses in a) indicate the most significant fire metric (N= number of fires; A= area burnt). Region codes: CHMEDI= Mediterranean Chile, WMEDIAUS= western Mediterranean Australia, EMEDIAUS= eastern Mediterranean Australia, SAFR= Mediterranean South Africa, SEAUS= temperate southeast Australia, WTAS= western Tasmania, TEMPSA= temperate South America (Chile and Argentina). The letter  $n$  in parentheses indicates the number of years used to run Pearson correlation coefficients. N/A stands for information Not Available due to lack of data. Control variables refers to the climate modes kept constant to account for co-dependencies in their respective effect on fire activity.

a) UNPLANNED FIRES (total of human- and lightning- ignited)								
			CONTROL VARIABLES: IOD + NIÑO3.4		CONTROL VARIABLES: IOD + SAM		CONTROL VARIABLES: SAM + NIÑO3.4	
			SAM	SAM SEASON	NIÑO3.4	NIÑO3.4 SEASON	IOD	IOD SEASON
Mediterranean	CHMEDI (n=26)	herbaceous	0.559 (0.005)	WINTER (A)	0.5722 (0.004)	ANNUAL (A)	-0.4860 (0.018)	WINTER (A)
		woody	0.4497 (0.024)	WINTER (A)	0.385 (0.069)	AUTUMN (A)	-0.3901 (0.065)	WINTER (A)
	WMEDIAUS (n=67)	herbaceous	0.4116 (0.0019)	SUMMER (N)	-0.2676 (0.05)	SPRING (N)	0.364 (0.006)	SPRING (N)
		woody	0.3017 (0.026)	ANNUAL (N)	0.2759 (0.043)	AUTUMN (A)	0.291 (0.03)	SPRING (N)
	EMEDIAUS (n=67)	herbaceous	-0.333 (0.013)	SPRING (A)	/	/	/	/
		woody	/	/	/	/	-0.2596 (0.057)	SUMMER (A)
SAFR (n=66)	woody	0.42 (0.001)	ANNUAL (N)	/	/	0.354 (0.008)	SPRING (N)	
Temperate	SEAUS (n=64)	herbaceous	-0.293 (0.031)	SPRING (A)	0.299 (0.027)	SPRING (A)	0.265 (0.05)	ANNUAL (N)
		woody	-0.3778 (0.004)	SPRING (A)	0.4217 (0.001)	SUMMER (A)	0.29 (0.03)	ANNUAL (N)
	WTAS (n=35)	herbaceous	0.4843 (0.0036)	SUMMER (N)	/	/	/	/
		woody	0.5601 (0.0005)	SUMMER (N)	0.3218 (0.063)	SUMMER (N)	0.3424 (0.04)	AUTUMN (N)
	TEMPSA (n=67)	herbaceous	0.4320 (0.001)	SUMMER (A)	/	/	0.309 (0.022)	SPRING (N)
		woody	0.4848 (0.0002)	SUMMER (N)	-0.2362 (0.085)	SPRING (A)	0.315 (0.03)	SPRING (A)
b) NUMBER OF LIGHTNING-LIT FIRES (summed occurrences; woody and herbaceous vegetation types combined)								
			CONTROL VARIABLES: IOD + NIÑO3.4		CONTROL VARIABLES: IOD + SAM		CONTROL VARIABLES: SAM + NIÑO3.4	
			SAM	SAM SEASON	NIÑO3.4	NIÑO3.4 SEASON	IOD	IOD SEASON
Mediterranean	CHMEDI (n=26)		0.3774 (0.075)	WINTER	-0.586 (0.0032)	SUMMER	/	/
	WMEDIAUS (n=40)		0.3679 (0.006)	SUMMER	/	/	0.3225 (0.0173)	SPRING
	EMEDIAUS		N/A	N/A	N/A	N/A	N/A	N/A
	SAFR (n=61)		0.3298 (0.019)	ANNUAL	-0.237 (0.093)	WINTER	0.2767 (0.051)	SPRING
Temperate	SEAUS (n=54)		0.2912 (0.044)	SUMMER	0.2666 (0.0669)	SUMMER	0.30879 (0.023)	SPRING
	WTAS (n=35)		0.2873 (0.099)	ANNUAL	/	/	0.3680 (0.032)	SPRING
	TEMPSA (n=67)		0.2871 (0.035)	AUTUMN	-0.3329 (0.013)	SPRING	0.2508 (0.0672)	SPRING
c) SOUTHERN HEMISPHERE SUMMED OCCURRENCES								
1958-2014			CONTROL VARIABLES: IOD + NIÑO3.4		CONTROL VARIABLES: IOD + SAM		CONTROL VARIABLES: SAM + NIÑO3.4	
			SAM	SAM SEASON	NIÑO3.4	NIÑO3.4 SEASON	IOD	IOD SEASON
All unplanned wildfires (n=66)			0.4225 (0.00145)	SUMMER	/	/	0.3264 (0.016)	SPRING
All lightning-ignited wildfires (n=66)			0.3295 (0.0147)	ANNUAL	/	/	0.3823 (0.0043)	SPRING

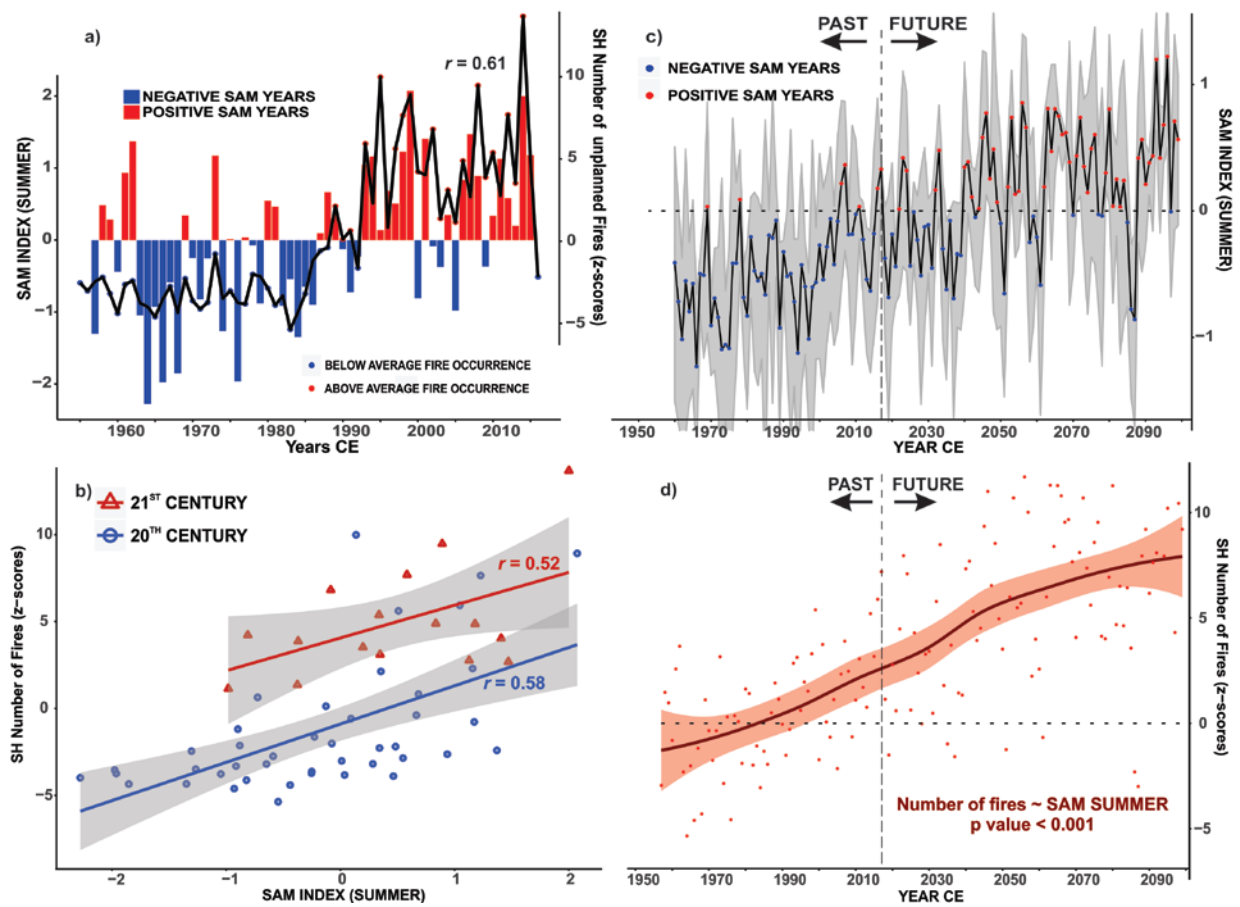


**Figure 2 a)** Stacked plots of the SAM Index (summer) and the total number of wildfires in the Southern Hemisphere (black solid line; only regions with a positive correlation with the SAM Index are included in the summed record) from all ignition sources and vegetation types combined; **b)** Scatterplot of the two time-series shown in a). Colour and symbol coding refers to the 20<sup>th</sup> (blue dots) and the 21<sup>st</sup> (red triangle) centuries; **c)** Summer SAM Index projection under increasing greenhouse gases concentrations (data from Thompson et al., 2011 and *McLandress et al.*, 2011); **d)** Linear model projecting the total (human and lightning-lit) wildfire occurrences in the SH extending to the year 2100 based on the SAM Index projection presented in c). Pearson correlation coefficients are reported in a) and b).

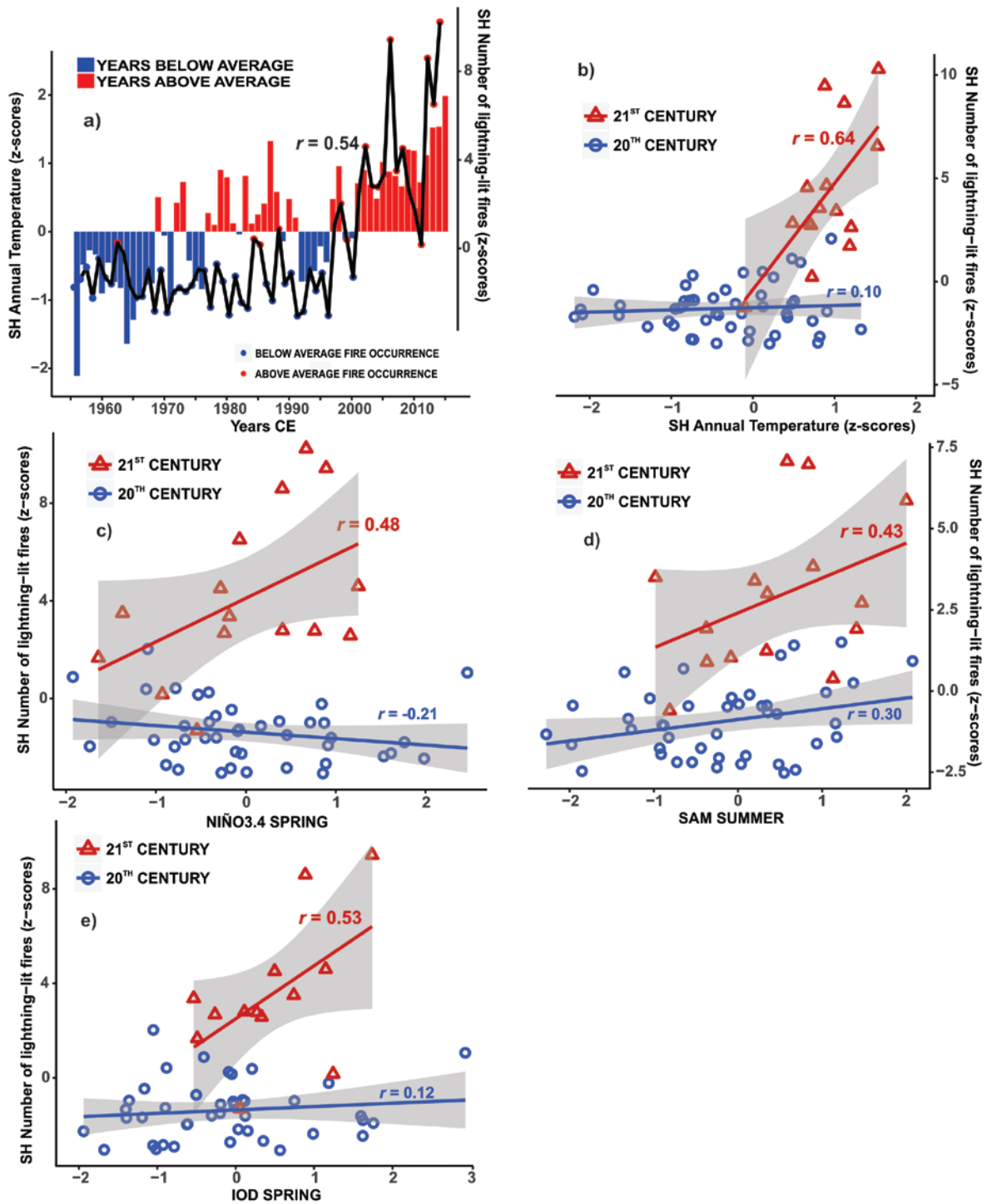


**Figure 3** **a)** Stacked plots of the SH annual temperatures (z-scores; data from ERA-Interim Reanalysis) and the total number of lightning-lit fires recorded in the Southern Hemisphere. **b)** Scatterplot of the SH annual temperatures (z-scores; data from ERA-

Interim Reanalysis) and the total number of lightning-lit fires recorded in the Southern Hemisphere; Black solid line in a) represents the summed SH number of lightning-ignited fires. Colour and symbol coding in b,c,d,e refers to the 20<sup>th</sup> (blue dots) and the 21<sup>st</sup> (red triangle) centuries. **c)** Scatterplot of the NIÑO3.4 Index (spring) and the number of lightning-lit fires across the SH; **d)** Scatterplot of the SAM Index (summer) and the number of lightning-lit fires across the SH; **e)** Scatterplot of the IOD Index (spring) and the number of lightning-lit fires across the SH.

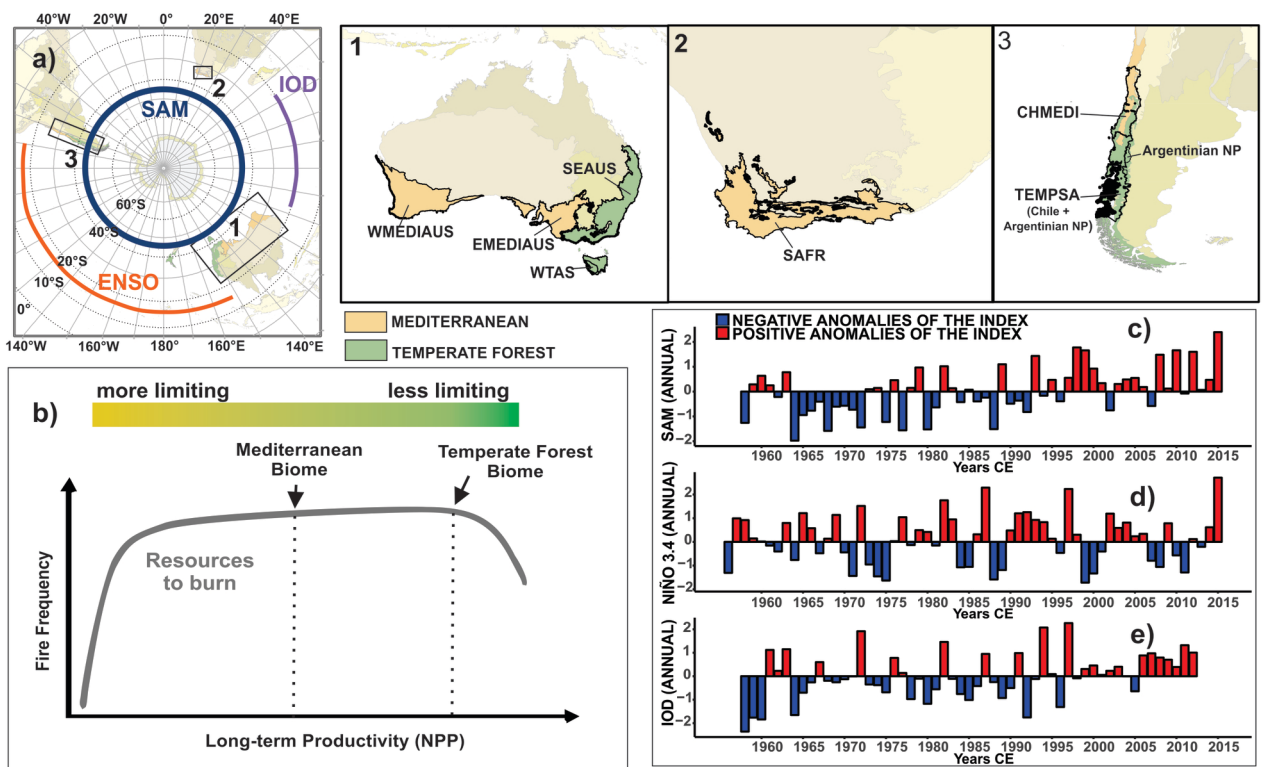
## REFERENCES

- Abatzoglou, J. T., and A. P. Williams (2016), Impact of anthropogenic climate change on wildfire across western US forests, *Proceedings of the National Academy of Sciences*, *113*(42), 11770-11775.
- Abatzoglou, J. T., C. A. Kolden, J. K. Balch, and B. A. Bradley (2016), Controls on interannual variability in lightning-caused fire activity in the western US, *Environmental Research Letters*, *11*(4), 045005.
- Abram, N. J., R. Mulvaney, F. Vimeux, S. J. Phipps, J. Turner, and M. H. England (2014), Evolution of the Southern Annular Mode during the past millennium, *Nature Climate Change*.
- Balch, J. K., B. A. Bradley, J. T. Abatzoglou, R. C. Nagy, E. J. Fusco, and A. L. Mahood (2017), Human-started wildfires expand the fire niche across the United States, *Proceedings of the National Academy of Sciences*, *114*(11), 2946-2951.
- Bond, W. J., F. I. Woodward, and G. F. Midgley (2005), The global distribution of ecosystems in a world without fire, *New Phytologist*, *165*(2), 525-537.
- Bowman, D. M., G. J. Williamson, J. T. Abatzoglou, C. A. Kolden, M. A. Cochrane, and A. M. Smith (2017), Human exposure and sensitivity to globally extreme wildfire events, *Nature Ecology & Evolution*, *1*, 0058.
- Bowman, D. M. J. S., et al. (2009), Fire in the Earth System, *Science*, *324*(5926), 481-484.
- Bradstock, R. A. (2010), A biogeographic model of fire regimes in Australia: current and future implications, *Global Ecology and Biogeography*, *19*, 145-158.
- Cai, W., T. Cowan, and M. Raupach (2009), Positive Indian Ocean dipole events precondition southeast Australia bushfires, *Geophysical Research Letters*, *36*(19).
- Cai, W., A. Sullivan, and T. Cowan (2011), Interactions of ENSO, the IOD, and the SAM in CMIP3 Models, *Journal of Climate*, *24*(6), 1688-1704.
- Cai, W., S. Borlace, M. Lengaigne, P. Van Rensch, M. Collins, G. Vecchi, A. Timmermann, A. Santoso, M. J. McPhaden, and L. Wu (2014), Increasing frequency of extreme El Niño events due to greenhouse warming, *Nature climate change*, *4*(2), 111-116.
- Cai, W., G. Wang, A. Santoso, M. J. McPhaden, L. Wu, F.-F. Jin, A. Timmermann, M. Collins, G. Vecchi, and M. Lengaigne (2015), Increased frequency of extreme La Niña events under greenhouse warming, *Nature Climate Change*, *5*(2), 132-137.

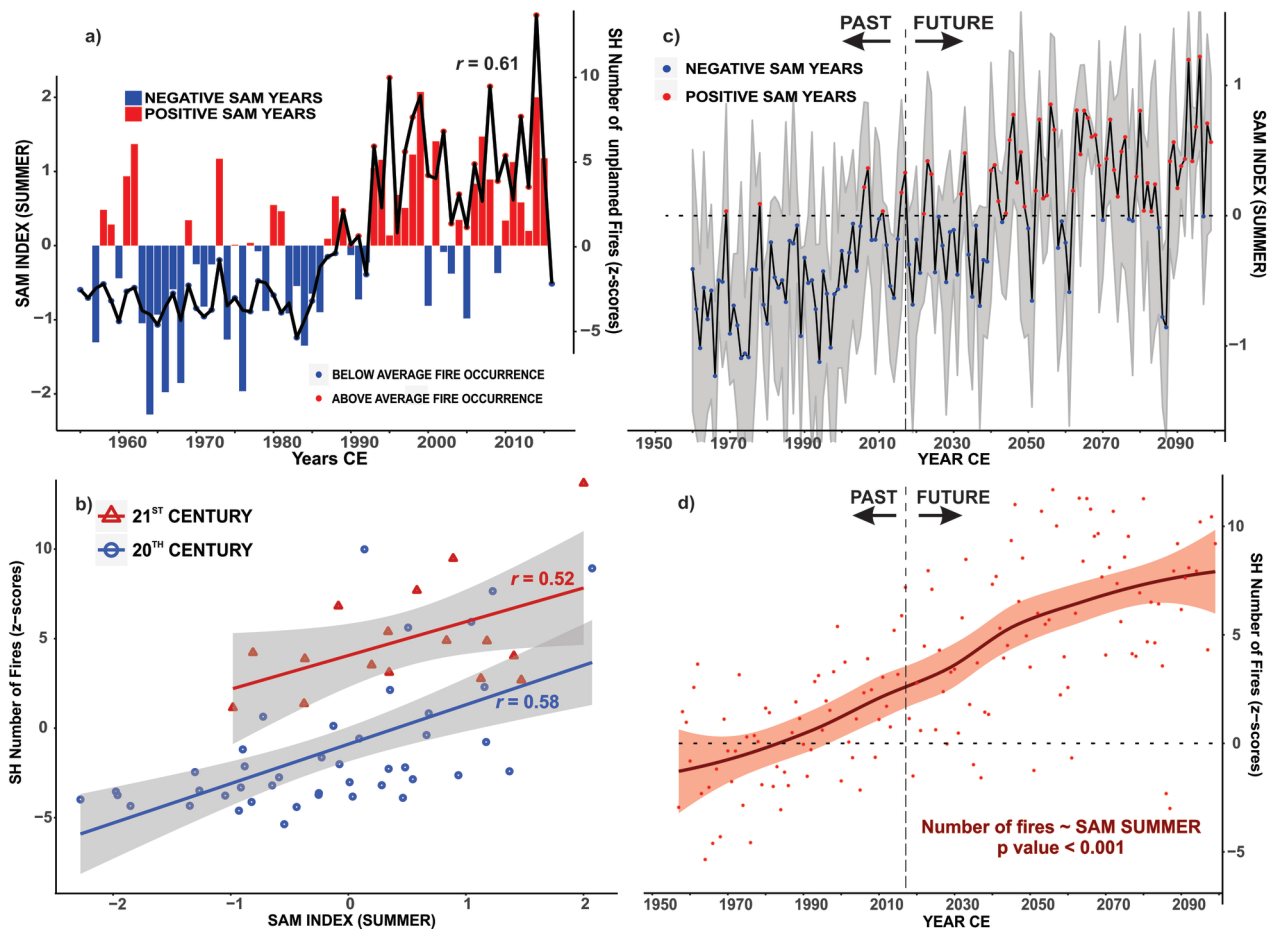
- Chan, S. C., S. K. Behera, and T. Yamagata (2008), Indian Ocean Dipole influence on South American rainfall, *Geophysical Research Letters*, 35(14), n/a-n/a.
- Cochrane, M. A. (2003), Fire science for rainforests, *Nature*, 421(6926), 913-919.
- Enright, N. J., and R. S. Hill (1995), Ecology of the southern conifers.
- Enright, N. J., J. B. Fontaine, D. M. Bowman, R. A. Bradstock, and R. J. Williams (2015), Interval squeeze: altered fire regimes and demographic responses interact to threaten woody species persistence as climate changes, *Frontiers in Ecology and the Environment*, 13(5), 265-272.
- Fogt, R. L., J. Perlwitz, A. J. Monaghan, D. H. Bromwich, J. M. Jones, and G. J. Marshall (2009), Historical SAM variability. Part II: twentieth-century variability and trends from reconstructions, observations, and the IPCC AR4 models\*, *Journal of Climate*, 22(20), 5346-5365.
- Garreaud, R. D., C. Alvarez-Garreton, J. Barichivich, J. P. Boisier, C. Duncan, M. Galleguillos, C. LeQuesne, J. McPhee, and M. Zambrano-Bigiarini (2017), The 2010–2015 megadrought in central Chile: impacts on regional hydroclimate and vegetation, *Hydrology and Earth System Sciences*, 21(12), 6307.
- Goldammer, J. G., and C. Price (1998), Potential impacts of climate change on fire regimes in the tropics based on MAGICC and a GISS GCM-derived lightning model, *Climatic change*, 39(2), 273-296.
- Hennessy, K., C. Lucas, N. Nicholls, J. Bathols, R. Suppiah, and J. Ricketts (2005), Climate change impacts on fire-weather in south-east Australia *Rep.*
- Holz, A., and T. T. Veblen (2011), Variability in the Southern Annular Mode determines wildfire activity in Patagonia, *Geophysical Research Letters*, 38(14), L14710.
- Holz, A., and T. T. Veblen (2012), Wildfire activity in rainforests in western Patagonia linked to the Southern Annular Mode, *International Journal of Wildland Fire*, 21(2), 114-126.
- Holz, A., T. Kitzberger, J. Paritsis, and T. T. Veblen (2012), Ecological and climatic controls of modern wildfire activity patterns across southwestern South America, *Ecosphere*, 3(11), 1-25.
- Holz, A., S. W. Wood, T. T. Veblen, and D. M. Bowman (2014), Effects of high severity fire drove the population collapse of the subalpine Tasmanian endemic conifer *Athrotaxis cupressoides*, *Global change biology*.
- Holz, A., J. Paritsis, I. A. Mundo, T. T. Veblen, T. Kitzberger, G. J. Williamson, E. Aráoz, C. Bustos-Schindler, M. E. González, and H. R. Grau (2017), Southern Annular Mode drives multicentury wildfire activity in southern South America, *Proceedings of the National Academy of Sciences*, 201705168.
- Jolly, W. M., M. A. Cochrane, P. H. Freeborn, Z. A. Holden, T. J. Brown, G. J. Williamson, and D. M. Bowman (2015), Climate-induced variations in global wildfire danger from 1979 to 2013, *Nature communications*, 6.
- Krause, A., S. Kloster, S. Wilkenskjeld, and H. Paeth (2014), The sensitivity of global wildfires to simulated past, present, and future lightning frequency, *Journal of Geophysical Research: Biogeosciences*, 119(3), 312-322.
- Krawchuk, M. A., M. A. Moritz, M.-A. Parisien, J. Van Dorn, and K. Hayhoe (2009), Global pyrogeography: the current and future distribution of wildfire, *PloS one*, 4(4), e5102.
- Liu, W., J. Lu, L. R. Leung, S.-P. Xie, Z. Liu, and J. Zhu (2015), The de-correlation of westerly winds and westerly-wind stress over the Southern Ocean during the Last Glacial Maximum, *Climate Dynamics*, 1-12.
- Mariani, M., and M. S. Fletcher (2016), The Southern Annular Mode determines inter - annual and centennial - scale fire activity in temperate southwest Tasmania, Australia, *Geophysical Research Letters*, 43(4), 1702-1709.

- Mariani, M., M. S. Fletcher, A. Holz, and P. Nyman (2016), ENSO controls interannual fire activity in southeast Australia, *Geophysical Research Letters*, 43(20), 10,891–810,900.
- McLandsress, C., T. G. Shepherd, J. F. Scinocca, D. A. Plummer, M. Sigmond, A. I. Jonsson, and M. C. Reader (2011), Separating the dynamical effects of climate change and ozone depletion. Part II: Southern Hemisphere troposphere, *Journal of Climate*, 24(6), 1850-1868.
- McWethy, D., P. Higuera, C. Whitlock, T. Veblen, D. Bowman, G. Cary, S. Haberle, R. Keane, B. Maxwell, and M. McGlone (2013), A conceptual framework for predicting temperate ecosystem sensitivity to human impacts on fire regimes, *Global Ecology and Biogeography*, 22(8), 900-912.
- Meyers, G., P. McIntosh, L. Pigot, and M. Pook (2007), The years of El Niño, La Niña, and interactions with the tropical Indian Ocean, *Journal of Climate*, 20(13), 2872-2880.
- Michalon, N., A. Nassif, T. Saouri, J. Royer, and C. Pontikis (1999), Contribution to the climatological study of lightning, *Geophysical research letters*, 26(20), 3097-3100.
- Moritz, M. A., M.-A. Parisien, E. Batllori, M. A. Krawchuk, J. Van Dorn, D. J. Ganz, and K. Hayhoe (2012), Climate change and disruptions to global fire activity, *Ecosphere*, 3(6), art49.
- Murphy, B. P., R. A. Bradstock, M. M. Boer, J. Carter, G. J. Cary, M. A. Cochrane, R. J. Fensham, J. Russell - Smith, G. J. Williamson, and D. M. Bowman (2013), Fire regimes of Australia: a pyrogeographic model system, *Journal of Biogeography*, 40(6), 1048-1058.
- Nicholls, N., and C. Lucas (2007), Interannual variations of area burnt in Tasmanian bushfires: relationships with climate and predictability, *International Journal of Wildland Fire*, 16(5), 540-546.
- Paritsis, J., T. T. Veblen, and A. Holz (2015), Positive fire feedbacks contribute to shifts from *Nothofagus pumilio* forests to fire - prone shrublands in Patagonia, *Journal of Vegetation Science*, 26(1), 89-101.
- Pausas, J. G., and E. Ribeiro (2013), The global fire–productivity relationship, *Global Ecology and Biogeography*, 22(6), 728-736.
- Power, S., F. Delage, C. Chung, G. Kociuba, and K. Keay (2013), Robust twenty-first-century projections of El Niño and related precipitation variability, *Nature*, 502(7472), 541-545.
- Price, C., and D. Rind (1994), Possible implications of global climate change on global lightning distributions and frequencies, *Journal of Geophysical Research: Atmospheres*, 99(D5), 10823-10831.
- Risbey, J. S., M. J. Pook, P. C. McIntosh, M. C. Wheeler, and H. H. Hendon (2009), On the remote drivers of rainfall variability in Australia, *Monthly Weather Review*, 137(10), 3233-3253.
- Romps, D. M., J. T. Seeley, D. Vollaro, and J. Molinari (2014), Projected increase in lightning strikes in the United States due to global warming, *Science*, 346(6211), 851-854.
- Saji, N., B. Goswami, P. Vinayachandran, and T. Yamagata (1999), A dipole mode in the tropical Indian Ocean, *Nature*, 401(6751), 360-363.
- Shapiro, S. S., and M. B. Wilk (1965), An analysis of variance test for normality (complete samples), *Biometrika*, 52(3/4), 591-611.
- Sharples, J. J., G. J. Cary, P. Fox-Hughes, S. Mooney, J. P. Evans, M.-S. Fletcher, M. Fromm, P. F. Grierson, R. McRae, and P. Baker (2016), Natural hazards in Australia: extreme bushfire, *Climatic Change*, 139(1), 85-99.
- Taschetto, A. S., and T. Ambrizzi (2012), Can Indian Ocean SST anomalies influence South American rainfall?, *Climate dynamics*, 38(7-8), 1615-1628.
- Team, R. C. D. (2013), R: A language and environment for statistical computing, in *R Foundation for Statistical Computing* edited, Vienna Austria.

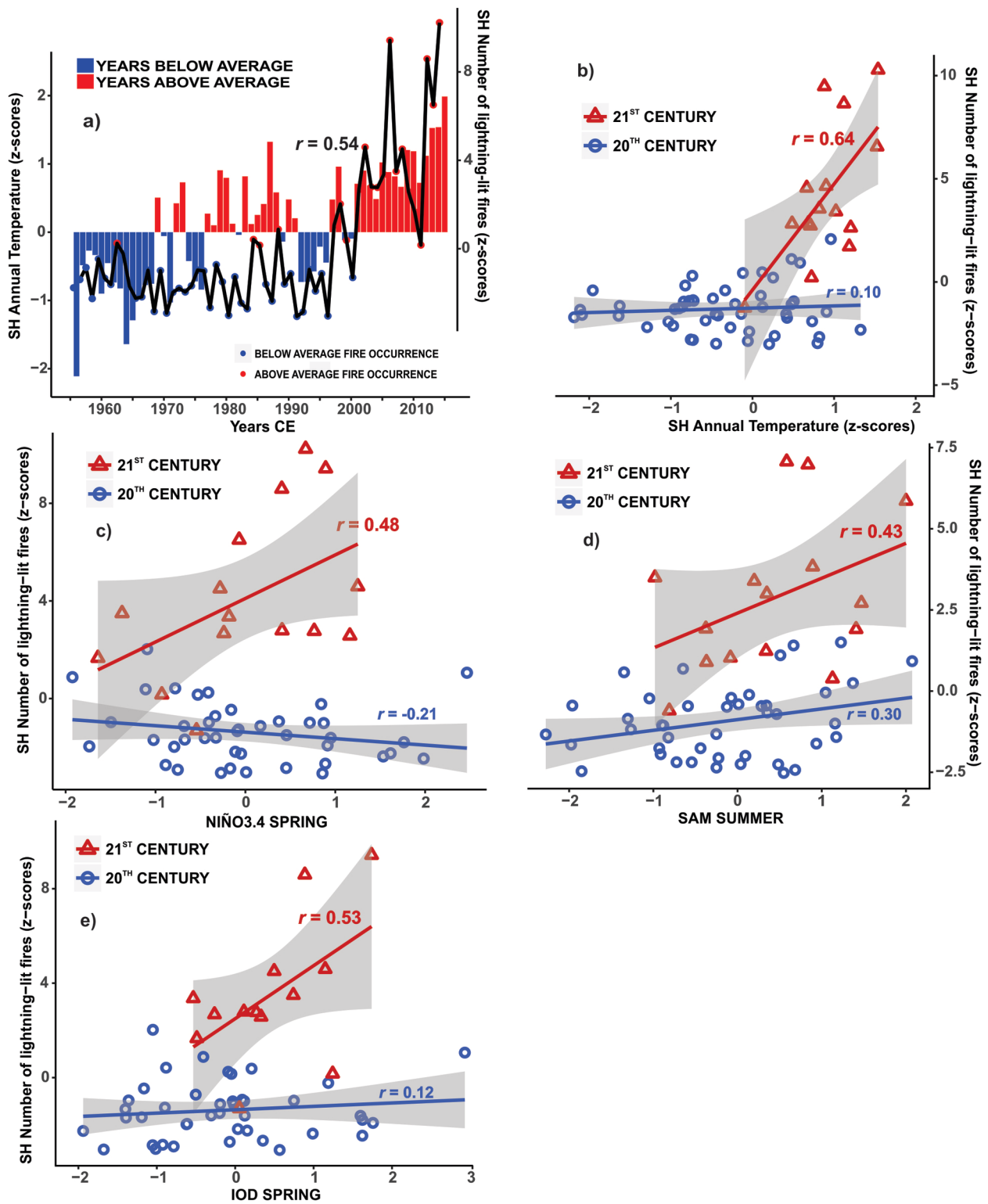
- Tepley, A. J., J. R. Thompson, H. E. Epstein, and K. J. Anderson - Teixeira (2017), Vulnerability to forest loss through altered postfire recovery dynamics in a warming climate in the Klamath Mountains, *Global Change Biology*.
- Tepley, A. J., E. Thomann, T. T. Veblen, G. L. Perry, A. Holz, J. Paritsis, T. Kitzberger, and K. J. Anderson - Teixeira (2018), Influences of fire-vegetation feedbacks and post - fire recovery rates on forest landscape vulnerability to altered fire regimes, *Journal of Ecology*.
- Thompson, D. W., S. Solomon, P. J. Kushner, M. H. England, K. M. Grise, and D. J. Karoly (2011), Signatures of the Antarctic ozone hole in Southern Hemisphere surface climate change, *Nature Geoscience*, 4(11), 741-749.
- Veblen, T. T., T. Kitzberger, R. Villalba, and J. Donnegan (1999), Fire history in northern Patagonia: the roles of humans and climatic variation, *Ecological Monographs*, 69(1), 47-67.
- Vecchi, G. A., and B. J. Soden (2007), Global warming and the weakening of the tropical circulation, *Journal of Climate*, 20(17), 4316-4340.
- Veraverbeke, S., B. M. Rogers, M. L. Goulden, R. R. Jandt, C. E. Miller, E. B. Wiggins, and J. T. Randerson (2017), Lightning as a major driver of recent large fire years in North American boreal forests, *Nature Climate Change*, 7(7), 529-534.
- Wei, T., and V. Simko (2016), corrplot: Visualization of a Correlation Matrix. R package version 0.77, CRAN, Vienna, Austria.
- Westerling, A. L., H. G. Hidalgo, D. R. Cayan, and T. W. Swetnam (2006), Warming and earlier spring increase western US forest wildfire activity, *science*, 313(5789), 940-943.
- Williams, E. (2005), Lightning and climate: A review, *Atmospheric Research*, 76(1), 272-287.



2018GL078294-f01-z-.jpg



2018GL078294-f02-z-.jpg



2018GL078294-f03-z-.jpg

a) UNPLANNED FIRES (total of human- and lightning- ignited)

	VEGETATION TYPE	CONTROL VARIABLES: IOD + NIÑO3.4		CONTROL VARIABLES: IOD + SAM		CONTROL VARIABLES: SAM + NIÑO3.4		
		SAM	SAM SEASON	NIÑO3.4	NIÑO3.4 SEASON	IOD	IOD SEASON	
Mediterranean	CHMEDI (n=26)	herbaceous	0.559 (0.005)	WINTER (A)	0.5722 (0.004)	ANNUAL (A)	-0.4860 (0.018)	WINTER (A)
		woody	0.4497 (0.024)	WINTER (A)	0.385 (0.069)	AUTUMN (A)	-0.3901 (0.065)	WINTER (A)
	WMEDIAUS (n=67)	herbaceous	0.4116 (0.0019)	SUMMER (N)	-0.2676 (0.05)	SPRING (N)	0.364 (0.006)	SPRING (N)
		woody	0.3017 (0.026)	ANNUAL (N)	0.2759 (0.043)	AUTUMN (A)	0.291 (0.03)	SPRING (N)
	EMEDIAUS (n=67)	herbaceous	-0.333 (0.013)	SPRING (A)	/	/	/	/
woody		/	/	/	/	-0.2596 (0.057)	SUMMER (A)	
SAFR (n=66)	woody	0.42 (0.001)	ANNUAL (N)	/	/	0.354 (0.008)	SPRING (N)	
Temperate	SEAUS (n=64)	herbaceous	-0.293 (0.031)	SPRING (A)	0.299 (0.027)	SPRING (A)	0.265 (0.05)	ANNUAL (N)
		woody	-0.3778 (0.004)	SPRING (A)	0.4217 (0.001)	SUMMER (A)	0.29 (0.03)	ANNUAL (N)
	WTAS (n=35)	herbaceous	0.4843 (0.0036)	SUMMER (N)	/	/	/	/
		woody	0.5601 (0.0005)	SUMMER (N)	0.3218 (0.063)	SUMMER (N)	0.3424 (0.04)	AUTUMN (N)
	TEMPSA (n=67)	herbaceous	0.4320 (0.001)	SUMMER (A)	/	/	0.309 (0.022)	SPRING (N)
woody		0.4848 (0.0002)	SUMMER (N)	-0.2362 (0.085)	SPRING (A)	0.315 (0.03)	SPRING (A)	

b) NUMBER OF LIGHTNING-LIT FIRES (summed occurrences; woody and herbaceous vegetation types combined)

	CONTROL VARIABLES: IOD + NIÑO3.4		CONTROL VARIABLES: IOD + SAM		CONTROL VARIABLES: SAM + NIÑO3.4		
	SAM	SAM SEASON	NIÑO3.4	NIÑO3.4 SEASON	IOD	IOD SEASON	
Mediterranean	CHMEDI (n=26)	0.3774 (0.075)	WINTER	-0.586 (0.0032)	SUMMER	/	/
	WMEDIAUS (n=40)	0.3679 (0.006)	SUMMER	/	/	0.3225 (0.0173)	SPRING
	EMEDIAUS	N/A	N/A	N/A	N/A	N/A	N/A
	SAFR (n=61)	0.3298 (0.019)	ANNUAL	-0.237 (0.093)	WINTER	0.2767 (0.051)	SPRING
Temperate	SEAUS (n=54)	0.2912 (0.044)	SUMMER	0.2666 (0.0669)	SUMMER	0.30879 (0.023)	SPRING
	WTAS (n=35)	0.2873 (0.099)	ANNUAL	/	/	0.3680 (0.032)	SPRING
	TEMPSA (n=67)	0.2871 (0.035)	AUTUMN	-0.3329 (0.013)	SPRING	0.2508 (0.0672)	SPRING

c) SOUTHERN HEMISPHERE SUMMED OCCURRENCES

1958-2014	CONTROL VARIABLES: IOD + NIÑO3.4		CONTROL VARIABLES: IOD + SAM		CONTROL VARIABLES: SAM + NIÑO3.4	
	SAM	SAM SEASON	NIÑO3.4	NIÑO3.4 SEASON	IOD	IOD SEASON
All unplanned wildfires (n=66)	0.4225 (0.00145)	SUMMER	/	/	0.3264 (0.016)	SPRING
All lightning-ignited wildfires (n=66)	0.3295 (0.0147)	ANNUAL	/	/	0.3823 (0.0043)	SPRING